Supporting Information:

Enhanced VOCs Recycling by Nano Fe/FeO_x Decorated Nano Porous Carbon

Weiping Zhang, [*ab] Xiong Xiao, [ab] Xiaoqin Wang, [ab] Hongli Liu, [ab] Xingye Zeng [c] and Taicheng An [ab]

[a] *Guangdong Key Laboratory of Environmental Catalysis and Health Risk Control, Guangdong-Hong Kong-Macao Joint Laboratory for Contaminants Exposure and Health, Institute of Environmental and Chemical Engineering Innovation, Institute of Environmental Health and Pollution Control, Guangdong University of Technology, Guangzhou 510006, China*

[b] *National Engineering Laboratory for VOCs Pollution Control Material & Technology Guangdong Branch, Guangdong Basic Research Center of Excellence for Ecological Security and Green Development, Guangdong Engineering Technology Research Centre for Photocatalytic Technology Integration and Equipment, School of Environmental Science and Engineering, Guangdong University of Technology, Guangzhou 510006, China.*

[c] *School of Chemical Engineering, Guangdong University of Petrochemical Technology, Maoming, 525000, P. R. China.*

***Corresponding Author:**

Assoc. Prof. Weiping Zhang; E-mail: wp.zhang86@gdut.edu.cn

Table of contents

Experiments

Materials:

Bacterial cellulose was purchased from Guilin Qihong Technology Store (Guangxi, China). Ferric acetate ($C_4H_7FeO_5 \cdot nH_2O$), ethanol (C_2H_6O, 95%) and sucrose were purchased from Macklin Biochemical Co., Ltd. Hydrochloric acid (HCl>98.0%), sodium hydroxide (NaOH), sodium bicarbonate ($NaHCO_3$, 99%), sodium carbonate (Na_2CO_3, 99%) were purchased from Guangzhou Weigu Technology Co., Ltd (Guangzhou, China). The standard ethyl acetate (EA) and toluene gas were purchased from Foshan Deli MESSER Gas Co., Ltd (Foshan, China). All of the chemical reagents were analytical-grade and used as received without further purification. Deionized water was used throughout the experiments.

Evaluation of Adsorption performance:

The adsorption experiments were carried out in a circular quartz reactor with a fixed bed at room temperature. To eliminate moisture and contaminants from the material, the adsorbents (20 ± 0.1 mg) were typically processed at 150°C for 1 h under vacuum before cooling to ambient temperature in a N_2 flow. The N_2 gas flow rate utilized as the EA and toluene carrier in the gas-phase adsorption process was kept constant at 30 mL min^{-1} to keep the inflow concentration of EA and toluene at 40 ppm (7% fluctuations). The EA and toluene content in the output gas was then continually measured using an online gas chromatograph equipped with a flame ionization detector. The adsorption capacity was determined by the difference between inlet and outlet VOC concentration. When the adsorption bed layer was saturated, the adsorption amount (q, mg g^{-1}) was calculated as follows[1]:

$$q = \frac{Q}{m * 10^{-6}} \int_0^{t_s} (C_{in} - C_{out}) dt$$

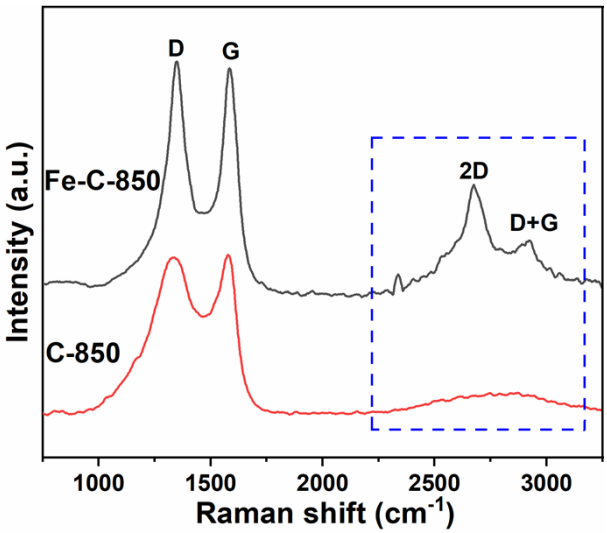

Fig. S1. Raman spectra of Fe-C-850 and C-850 adsorbents.

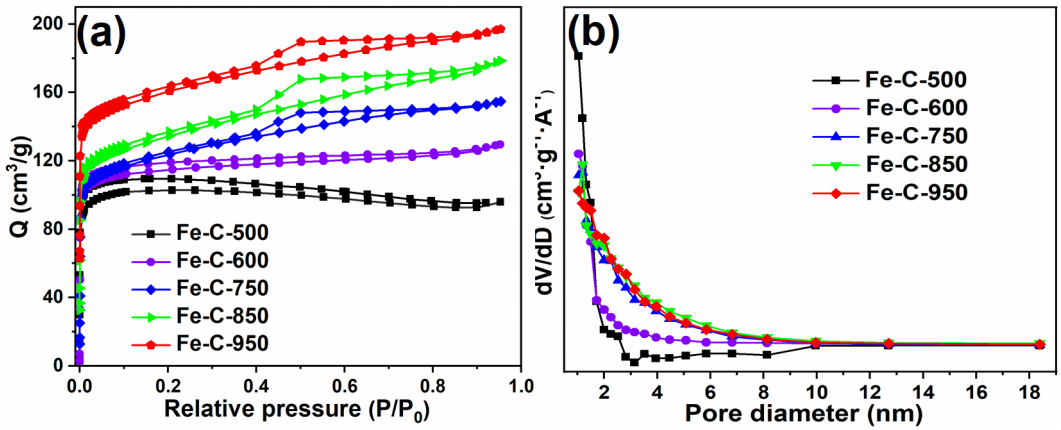

Fig. S2. N_2 adsorption-desorption isotherms and pore distribution of Fe-C composites synthesized at different pyrolysis temperatures.

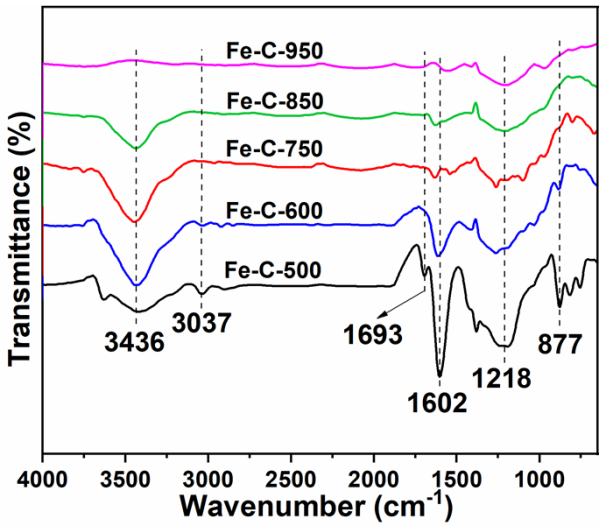

Fig. S3. FT-IR spectra of Fe-C composites synthesized at different pyrolysis temperature.

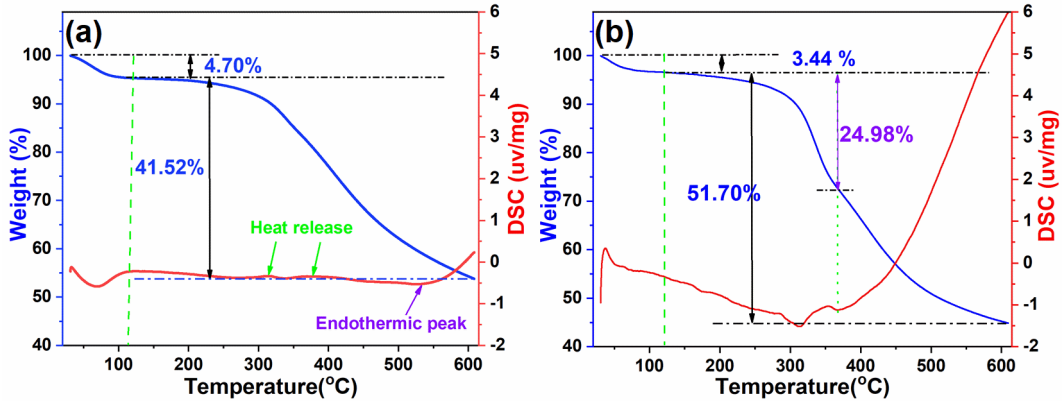

Fig. S4. TG-DSC curves of organic dry gel precursor pyrolyzed with argon gas protection (a, pure carbon gel precursor; b, Fe-C composite gel precursor).

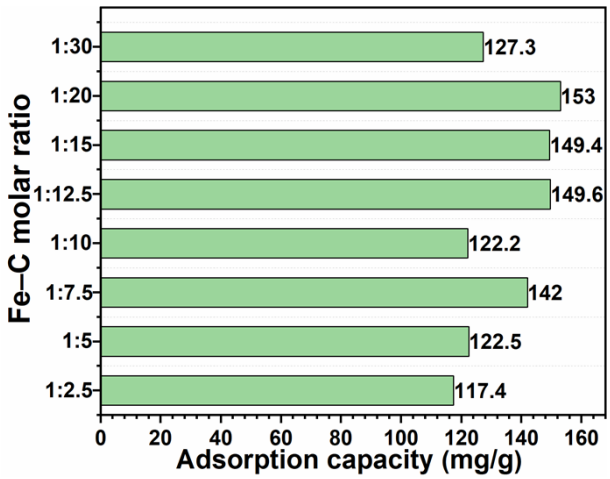

Fig. S5. Adsorption capacity of Fe-C composites with different Fe-C molar ratios at pyrolysis temperatures of 600 ℃. The adsorption capacity increased significantly to 153 mg·g^{-1} as the molar ratio of Fe to C decreased from 1:2.5 to 1:20. However, the adsorption capacity started to decrease gradually to 127.3 mg·g^{-1} as the molar ratio further decreased from 1:20 to 1:30.

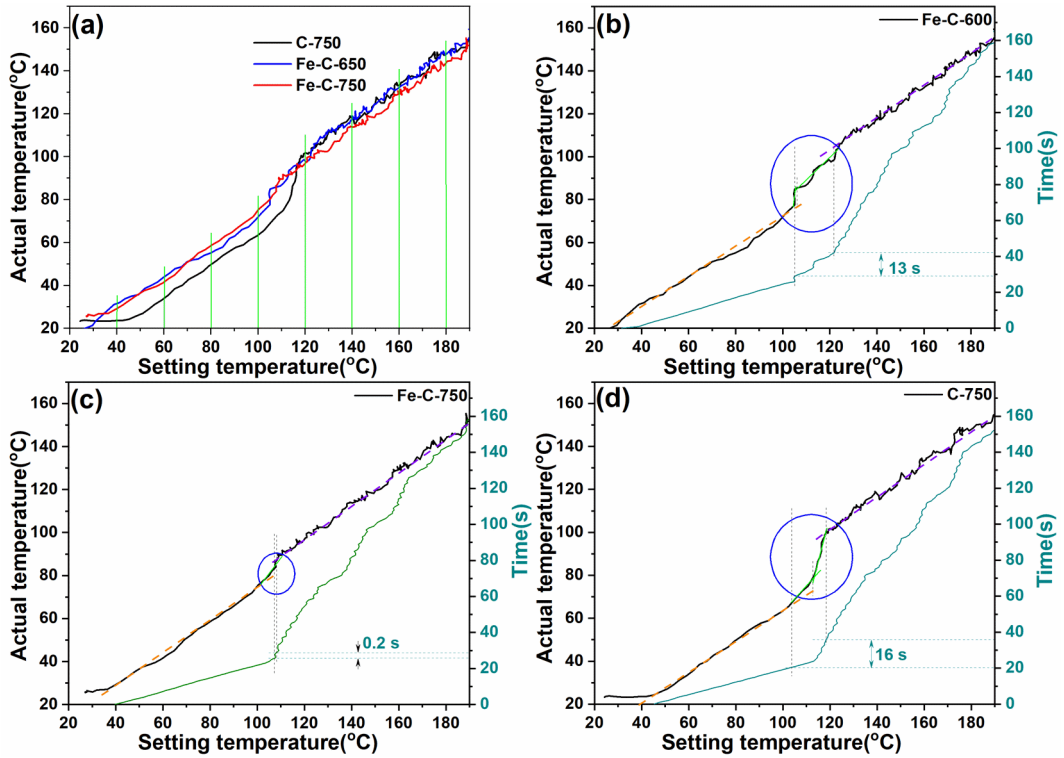

Fig. S6. Time-temperature variation curve of Fe-C-600, Fe-C-750 and C-750 adsorbents.

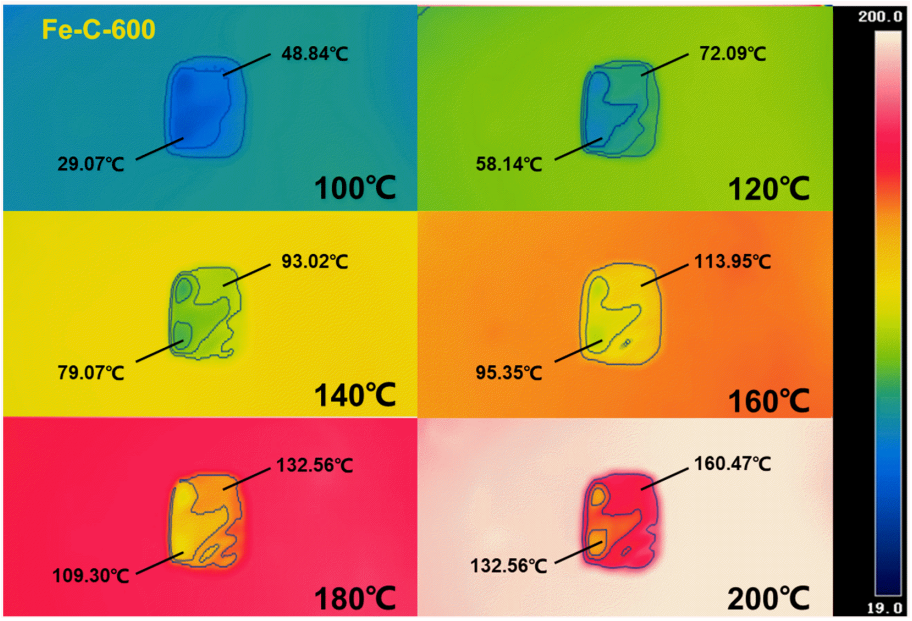

Fig. S7. Infrared thermal image of Fe-C-600 adsorbents.

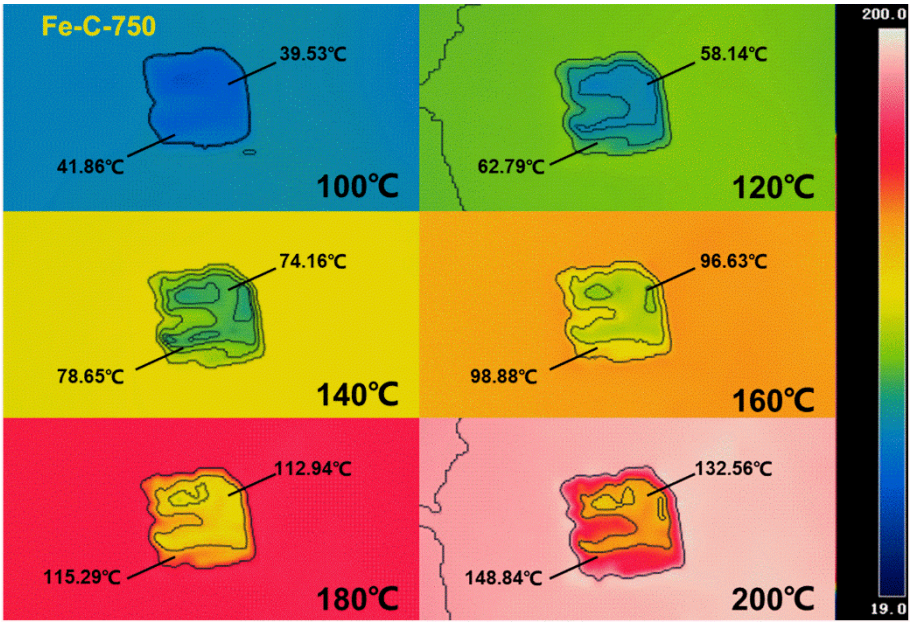

Fig. S8. Infrared thermal image of Fe-C-750 adsorbents.

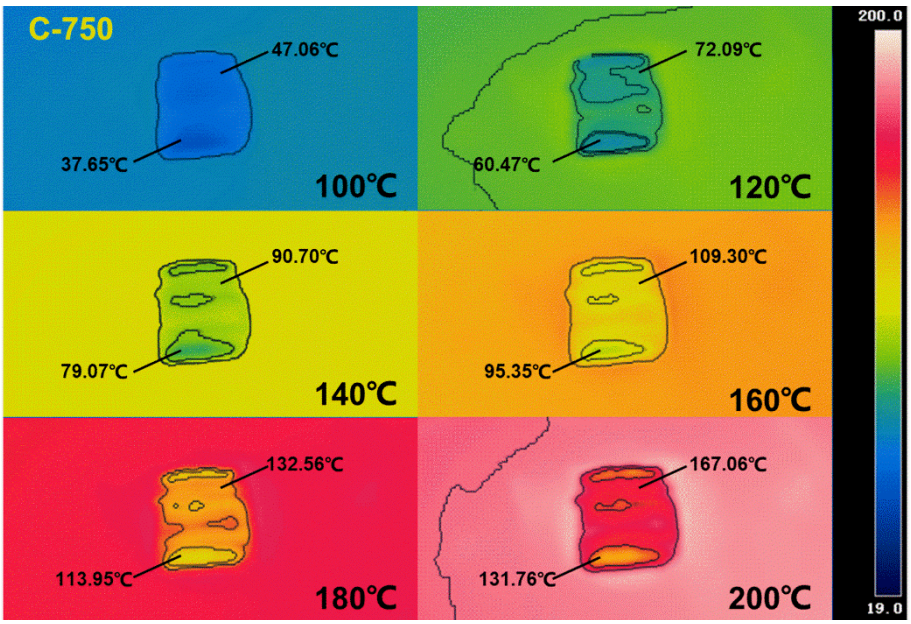

Fig. S9. Infrared thermal image of C-750 adsorbents.

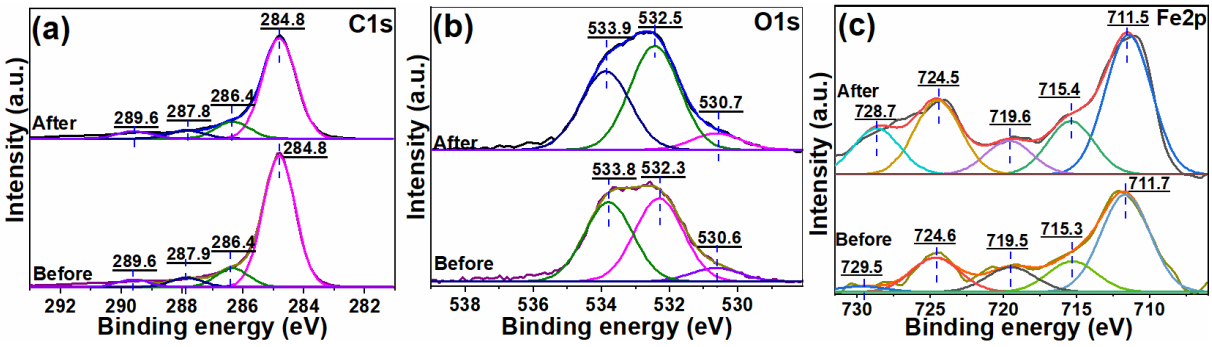

Fig. S10. High resolution X-ray photoelectron spectroscopy (XPS) spectra of C1s (a), O1s (b) and Fe2p (c) before and after EA adsorption by Fe-C-600.

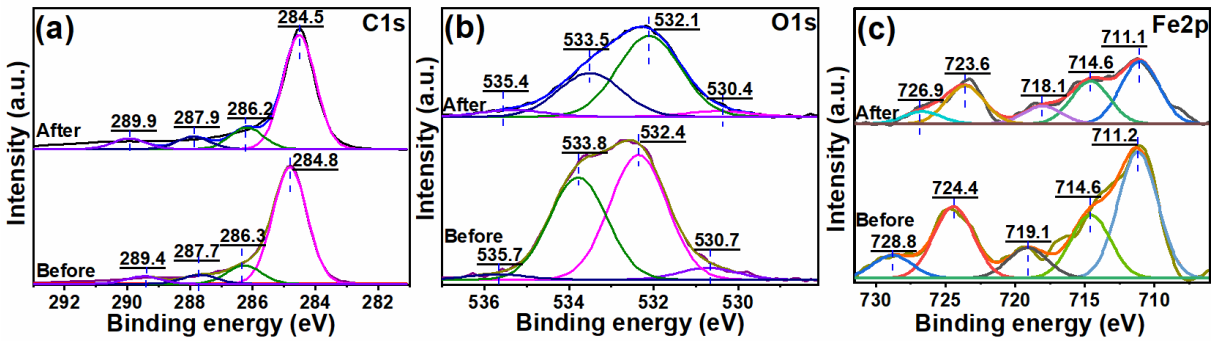

Fig. S11. High resolution X-ray photoelectron spectroscopy (XPS) spectra of C1s (a), O1s (b) and Fe2p (c) before and after toluene adsorption by Fe-C-750.

Table S1. I_D/I_G of the tested Fe-C composites by the deconvolution of Raman spectra.

Sample name	I_D/I_G
Fe-C-500	1.95
Fe-C-600	1.74
Fe-C-750	1.48
Fe-C-850	1.44
Fe-C-950	1.41
C-850	2.70

Table S2. Porous structure and specific surface area of the tested Fe-C composites.

Sample name	D_{BET} (nm)	S_{BET} ($m^2 \bullet g^{-1}$)	*Porosity Distribution by DFT Model*		
			V_{total} ($mL \bullet g^{-1}$)	V_{mic} ($mL \bullet g^{-1}$)	$V_{meso+Mac}$ ($mL \bullet g^{-1}$)
Fe-C-500	1.94	306.37	0.15	0.061	0.089
Fe-C-600	2.30	348.28	0.20	0.10	0.10
Fe-C-750	2.48	361.30	0.22	0.064	0.17
Fe-C-850	2.72	338.12	0.23	0.056	0.17
Fe-C-950	2.60	326.20	0.21	0.056	0.16
C-750	3.41	163.66	0.14	0.063	0.079

Table S3. Concentration of oxygen-containing groups of Fe-C composites measured by a Boehm's titration quantitative method.

Samples	Concentration of oxygen-containing groups (μmmol g^{-1})				
	Carboxylic group	**Phenolic group**	**Lactonic group**	**Basic group**	**Total**
Fe-C-500	0.286	1.234	0.269	3.293	5.082
Fe-C-600	0.0930	1.217	0.265	3.520	5.095
Fe-C-750	0.0716	0.350	0.867	3.293	4.582
Fe-C-850	0.0357	0.143	0.608	2.611	3.398
Fe-C-950	0.0710	0.215	0.429	3.564	4.279

Table S4. Spearman correlations of EA adsorption with pore structure, functional groups and other factors.

	Q_{EA}	***T_p***	***W_{Fe}***	***S_{BET}***	**V_{total}**	**Carboxyl**	**Base**	**PhOH**	**Lactonyl**	***D_p***	***V_{mic}***	***V_{meso}***
Q_{EA}	1.00	-0.80	0.50	0.10	-0.80	0.90	0.36	0.90	-0.70	-0.90	1.00	-1.00
T_p	-0.80	1.00	-0.70	0.10	0.70	-0.90	0.21	-0.90	0.50	0.90	-0.80	0.80
W_{Fe}	0.50	-0.70	1.00	0.40	-0.20	0.60	-0.36	0.60	0.20	-0.60	0.50	-0.50
S_{BET}	0.10	0.10	0.40	1.00	0.50	-0.20	-0.10	-0.20	0.40	0.20	0.10	-0.10
V_{total}	-0.80	0.70	-0.20	0.50	1.00	-0.90	-0.46	-0.90	0.80	0.90	-0.80	0.80
Carboxyl	0.90	-0.90	0.60	-0.20	-0.90	1.00	0.21	1.00	-0.60	-1.00	0.90	-0.90
Base	0.36	0.21	-0.36	-0.10	-0.46	0.21	1.00	0.21	-0.46	-0.21	0.36	-0.36
PhOH	0.90	-0.90	0.60	-0.20	-0.90	1.00	0.21	1.00	-0.60	-1.00	0.90	-0.90
Lactonyl	-0.70	0.50	0.20	0.40	0.80	-0.60	-0.46	-0.60	1.00	0.60	-0.70	0.70
D_p	-0.90	0.90	-0.60	0.20	0.90	-1.00	-0.21	-1.00	0.60	1.00	-0.90	0.90
V_{mic}	1.00	-0.80	0.50	0.10	-0.80	0.90	0.36	0.90	-0.70	-0.90	1.00	-1.00
V_{meso}	-1.00	0.80	-0.50	-0.10	0.80	-0.90	-0.36	-0.90	0.70	0.90	-1.00	1.00

Footnote: Q=adsorption capacity/mg g^{-1}; T=temperature/^{o}C; concentration of Fe (C_{Fe})/wt%; Concentration of functional group/μmmol g^{-1}; S/ m^2 g^{-1}; pore volume(V)/mL g^{-1}

Table S5. Spearman correlations of toluene adsorption with pore structure, functional groups and other factors.

	Q_{tol}	T_p	W_{Fe}	S_{BET}	V_{total}	Carboxyl	Base	PhOH	Lactonyl	D_p	V_{mic}	V_{meso}
Q_{tol}	1.00	0.10	0.40	1.00	0.50	-0.20	-0.10	-0.20	0.40	0.20	0.10	-0.10
T_p	0.10	1.00	-0.70	0.10	0.70	-0.90	0.21	-0.90	0.50	0.90	-0.80	0.80
W_{Fe}	0.40	-0.70	1.00	0.40	-0.20	0.60	-0.36	0.60	0.20	-0.60	0.50	-0.50
S_{BET}	1.00	0.10	0.40	1.00	0.50	-0.20	-0.10	-0.20	0.40	0.20	0.10	-0.10
V_{total}	0.50	0.70	-0.20	0.50	1.00	-0.90	-0.46	-0.90	0.80	0.90	-0.80	0.80
Carboxyl	-0.20	-0.90	0.60	-0.20	-0.90	1.00	0.21	1.00	-0.60	-1.00	0.90	-0.90
Base	-0.10	0.21	-0.36	-0.10	-0.46	0.21	1.00	0.21	-0.46	-0.21	0.36	-0.36
PhOH	-0.20	-0.90	0.60	-0.20	-0.90	1.00	0.21	1.00	-0.60	-1.00	0.90	-0.90
Lactonyl	0.40	0.50	0.20	0.40	0.80	-0.60	-0.46	-0.60	1.00	0.60	-0.70	0.70
D_p	0.20	0.90	-0.60	0.20	0.90	-1.00	-0.21	-1.00	0.60	1.00	-0.90	0.90
V_{mic}	0.10	-0.80	0.50	0.10	-0.80	0.90	0.36	0.90	-0.70	-0.90	1.00	-1.00
V_{meso}	-0.10	0.80	-0.50	-0.10	0.80	-0.90	-0.36	-0.90	0.70	0.90	-1.00	1.00

Footnote: Q=adsorption capacity/mg g^{-1}; T=temperature/^{o}C; concentration of Fe (C_{Fe}) /wt%; Concentration of functional group/μmmol g^{-1}; S/ m^2 g^{-1}; pore volume(V)/mL g^{-1}

Table S6. Proportion of functional groups on Fe-C-600 by deconvolution of XPS C1s, O1s and Fe2p spectra.

	Fe-C-600 before EA adsorption				**Fe-C-600 after regeneration**			
	Peak/eV	Groups	Proportion/%	Total /%	Peak/eV	Groups	Proportion/%	Total /%
C1s	284.8	C-C	78.82	**85.29**	284.8	C-C	75.82	**80.34**
	286.4	C-OH	11.23		286.4	C-OH	12.68	
	287.9	C-O	5.56		287.8	C-O	6.18	
	289.6	C=O	4.40		289.6	C=O	5.32	
O1s	530.6	C=O	7.65	**13.42**	530.7	C=O	7.57	**17.16**
	532.3	O=C-O-(C, O)	47.27		532.5	O=C-O-(C, O)	52.64	
	533.8	C-O-C	45.08		533.9	C-O-C	39.79	
Fe2p	724.6	1/2	25.9	**1.29**	724.5	1/2	34.7	**2.50**
	711.7	3/2	74.1		711.5	3/2	65.3	

Table S7. Proportion of functional groups on Fe-C-750 by deconvolution of XPS C1s, O1s and Fe2p spectra.

	Fe-C-750 before Toluene adsorption				**Fe-C-750 after regeneration**			
	Peak/eV	Groups	Proportion/%	Total /%	Peak/eV	Groups	Proportion/%	Total /%
C1s	284.8	C-C	76.97	**81.08**	284.5	C-C	72.16	**88.11**
	286.3	C-OH	12.20		286.2	C-OH	13.60	
	287.7	C-O	5.87		287.9	C-O	7.67	
	289.4	C=O	4.96		289.9	C=O	6.58	
O1s	530.7	C=O	4.72	**17.57**	530.4	C=O	3.94	**11.14**
	532.4	O=C-O-(C, O)	51.21		532.1	O=C-O-(C, O)	59.32	
	533.8	C-O-C	41.92		533.5	C-O-C	31.94	
	535.7	O=C-O-(C,O)	2.15		535.4	O=C-O-(C,O)	4.79	
Fe2p	724.4	1/2	36.16	**1.35**	723.6	1/2	37.86	**0.75**
	711.2	3/2	63.84		711.1	3/2	62.14	

Table S8. Adsorption and desorption performance of carbon materials as compared previous reports.

Adsorbent type	**Adsorption capacity**		**Regenerated performance**	**Regenerated temperature**	**reference**
	Toluene	**EA**	**--**	**--**	
Fe-C composites	200 $mg \cdot g^{-1}$	154 $mg \cdot g^{-1}$	100%	120 °C	This research
Nano-porous carbon	--	1.28~142 $mg \cdot g^{-1}$	63~88%	120 °C	[2]
HAT-650	--	140.98 $mg \cdot g^{-1}$	84.6%	120 °C	[3]
CAR-AC	--	61.5 $mg \cdot g^{-1}$	91.46%	120 °C	[1]
NHPC-CC	547 $mg \cdot g^{-1}$	--	93.69%	300 °C	[4]
Coffee ground-AC (BAC)	536 $mg \cdot g^{-1}$	--	94%	120 °C	[5]
$C_{0.1}$@HCS	813 $mg \cdot g^{-1}$	--	92.4%	200 °C	[6]

1. Yao, X.; Liu, Y.; Li, T.; Zhang, T.; Li, H.; Wang, W.; Shen, X.; Qian, F. and Yao, Z., *Journal of Hazardous Materials*, 2020, **392**, 122323.
2. Zhang, W.; Wang, X.; Pan, H.; Zeng, X.; Li, G.; Liu, H.; Kong, J.; Zhao, H. and An, T., *Environmental Science: Nano*, 2023, **10**, 2790-2798.
3. Tan, L.; Wang, J.; Cai, B.; Wang, C.; Ao, Z. and Wang, S., *Journal of Hazardous Materials*, 2022, **424**, 127348.
4. Huang, X.; Tang, M.; Li, H.; Wang, L. and Lu, S., *Chemosphere*, 2023, **313**, 137513.
5. Wang, S.; Xu, J.; Zhang, J.; Lyu, Y. and Chen, S., *Separation and Purification Technology*, 2024, **344**, 127269.
6. Qin, L.; Li, J.; Nestle Asamoah, E.; Zhao, B.; Chen, W. and Han, J., *Langmuir*, 2023, **39**, 6169-6177.